WORLD JOURNAL OF PHARMACEUTICAL RESEARCH
SJIF Impact Factor 8.453
Volume 14, Issue 19, 1059-1083. Research Article ISSN 2277–7105

SYNTHESIS, AND COMPUTATIONAL INVESTIGATION OF A 3,4-DIHYDROPYRIMIDINE-2(1*H*)-ONE DERIVATIVE: DFT, ADME, AND MOLECULAR DOCKING STUDIES

***Rajendra K. Pawar**

Department of Chemistry, Mahatma Gandhi Vidyamandir's Maharaja Sayajirao Gaikwad Arts, Science and Commerce College, Malegaon, Nashik 423105, Maharashtra, India, (Affiliated to Savitribai Phule Pune University, Pune, India).

Article Received on
18 August 2025,

Revised on 07 Sept. 2025,
Accepted on 27 Sept. 2025

https://doi.org/10.5281/zenodo.17277888

***Corresponding Author**
Rajendra K. Pawar
Department of Chemistry, Mahatma Gandhi Vidyamandir's Maharaja SayajiraoGaikwad Arts, Science and Commerce College, Malegaon, Nashik 423105, Maharashtra, India (Affiliated to Savitribai Phule Pune University, Pune, India).

ABSTRACT

A 3,4-dihydropyrimidine-2(1*H*)-one derivative was synthesized via a one-pot condensation reaction involving 4-nitrobenzaldehyde, urea, and ethyl acetoacetate, with sulfamic acid serving as a mild and eco-friendly catalyst in ethanol. The structure was confirmed by FT-IR, ^{1}H and ^{13}C NMR spectroscopy. Density Functional Theory (DFT) calculations at the B3LYP/6-311++G(d,p) level provided optimized geometries, bond lengths, bond angles, revealing a partially planar, conjugated framework stabilized by resonance across the pyrimidine, ester, and nitrophenyl moieties. Frontier molecular orbital analysis showed a HOMO–LUMO gap of 4.09 eV, suggesting moderate chemical reactivity. Molecular electrostatic potential (MEP) mapping identified regions of high electron density around electronegative atoms and electron-deficient zones over hydrogen atoms, providing insight into possible reactive sites and non-covalent interactions. In silico ADME evaluation predicted favorable pharmacokinetic and drug-likeness properties, including good solubility, high gastrointestinal absorption, and compliance with Lipinski's rule of five. Molecular docking revealed stable interactions with sterol 14-α demethylase (CYP51) and *E. coli* DNA gyrase B. Key interactions with CYP51 included a conventional hydrogen bond with TYR132, a carbon–hydrogen bond with ILE304, a π–donor hydrogen bond with TYR118, hydrophobic and π–alkyl interactions with PHE228 and HIS310, and a π–alkyl interaction with the heme group (HEM601). Docking with DNA

gyrase B showed π–cation interactions with ARG76, π–anion interactions with GLU50, and hydrophobic contacts with ILE78 and ILE94. These interactions suggest the compound's potential antifungal and antibacterial activity, highlighting it as a promising scaffold for further medicinal chemistry exploration.

KEYWORDS: 3,4-Dihydropyrimidine-2(1*H*)-one, DFT, FMO's, Molecular Docking, ADME.

1. INTRODUCTION

The alarming rise of multidrug-resistant microbial strains has created a significant challenge in modern medicine, highlighting the urgent need for new chemical entities with potent and broad-spectrum antimicrobial activity.[1-4] Heterocyclic compounds, especially nitrogen-containing scaffolds, have been widely explored due to their structural versatility and capacity to interact with diverse biological targets.[5-7] Among these, dihydropyrimidinones (DHPMs)1,2,3,4-tetrahydropyrimidine derivatives containing a 2-oxo functionalityhave attracted considerable attention owing to their broad spectrum of pharmacological properties.[8, 9] DHPMs are reported to exhibit antibacterial[10], antifungal[11], anticancer[12], anti-inflammatory[13], and antioxidant[14] activities, making them a privileged scaffold in drug discovery. The incorporation of substituents such as aryl groups at C4 and ester or carboxylate functionalities at C5, as well as small alkyl groups at C6, has been shown to significantly modulate the electronic distribution, lipophilicity, and hydrogen-bonding ability of these molecules, directly affecting their biological potency and selectivity. Multicomponent one-pot reactions (MCRs) have emerged as a highly efficient, sustainable, and versatile synthetic strategy for accessing DHPM derivatives.[15] In an MCR, three or more starting materials react simultaneously in a single reaction vessel to form the target molecule, which dramatically reduces reaction time, energy consumption, and the need for extensive purification, compared to conventional stepwise syntheses. This approach is highly advantageous for generating structurally diverse DHPM libraries, enabling rapid exploration of structure–activity relationships (SAR). Additionally, the use of MCRs aligns with the principles of green chemistry, promoting atom economy, minimizing waste, and improving overall synthetic efficiency. Consequently, MCRs have become a preferred method for the synthesis of biologically relevant DHPM derivatives, including those targeting microbial pathogens.

Alongside experimental synthesis, computational chemistry and *in silico* studies have become indispensable in modern drug discovery.[16-18] Density Functional Theory (DFT) was employed to optimize the geometry of the synthesized derivatives, providing the most energetically favourable conformation. Frontier molecular orbital (HOMO–LUMO) analysis, along with the calculation of electronic parameters and global reactivity descriptors, allowed the identification of reactive centers, evaluation of chemical stability, and assessment of the compound's potential for charge transfer processes.[19-22] These theoretical findings complement experimental characterization, enabling a deeper understanding of how structural modifications influence reactivity and bioactivity.To further explore biological potential, molecular docking studies were carried out to predict the binding orientation and affinity of the bioactive pharmacophore with microbial protein targets.[23-25] Docking simulations revealed the nature of key noncovalent interactionsincluding hydrogen bonds, π–π stacking, and hydrophobic contactsthat stabilize ligand–protein complexes and underpin biological activity. These results provide mechanistic insights into molecular recognition and guide structure–activity relationship (SAR) considerations. When coupled with ADME analysis, docking outcomes strengthen the evaluation of drug-likeness, pharmacokinetics, and therapeutic promise of therapeutic scaffolds.[26]

In the present study, we report the synthesis of a DHPM derivative, Ethyl 6-methyl-4-(4-nitrophenyl)-2-oxo-1,2,3,4-tetrahydropyrimidine-5-carboxylate, via a multicomponent one-pot reaction, affording a high yield and operational simplicity. The compound was characterized byspectral methods, confirming the DHPM core, aryl substitution, and ethyl ester group. Theoretical studies including geometry optimization, HOMO-LUMO analysis, electronic parameters, and global reactivity descriptors provided insight into its stability and reactive sites. Its antimicrobial potential was evaluated via molecular docking, and drug-likeness assessed through ADME analysis. This integrated approach underscores the promise of MCR-derived DHPMs as scaffolds for antimicrobial drug development.

2. EXPERIMENTAL

2.1. MATERIALS AND METHOD

The chemicals (Make-SD fine chemicals and Avra synthesis) were purchased fromthe high purity Sigma laboratory, Nashik, and were utilized accordingly. The NMR analysis was performed on advanced multinuclear FT-NMR Spectrometer model. In DMSO-d_6, the compounds were dissolved. Chemical shifts in ppm using tetramethylsilane (TMS) as an

internal standard were recorded. Thereactions were analyzed using thin-layer chromatography on a silica gel coated with fluorescent indicator F254 on the Merck Aluminium TLC plate. All the glass components were cleaned and dried in the oven prior to use.

2.2 General methodology for the synthesis of 3,4-dihydropyrimidine-2(1*H*)-one derivatives

A mixture of aromatic aldehyde (**1,**1 mmol), urea (**2**, 1mmol), ethyl acetoacetate (**3**, 1 mmol) and sulfamic acid (15 mol %) were mixed in a 50 ml conical flask containing ethyl alcohol as a solvent. This mixture was stirred at 70 °C for an appropriate time. The mixture is then cooled to room temperature after completion of reaction (monitored by TLC). After cooling to room temperature, the reaction mixture was poured onto crushed ice. The precipitate was filtered under suction, washed with water, dried and recrystallized from ethanol to afford the desired dihydropyrimidinones. Using FT-IR, ^{1}HNMR and ^{13}C NMR spectral techniques, the synthesized product were characterized. The synthesis of 3,4 dihydropyrimidine-2(1*H*)-one derivative is depicted in **Scheme 1**.

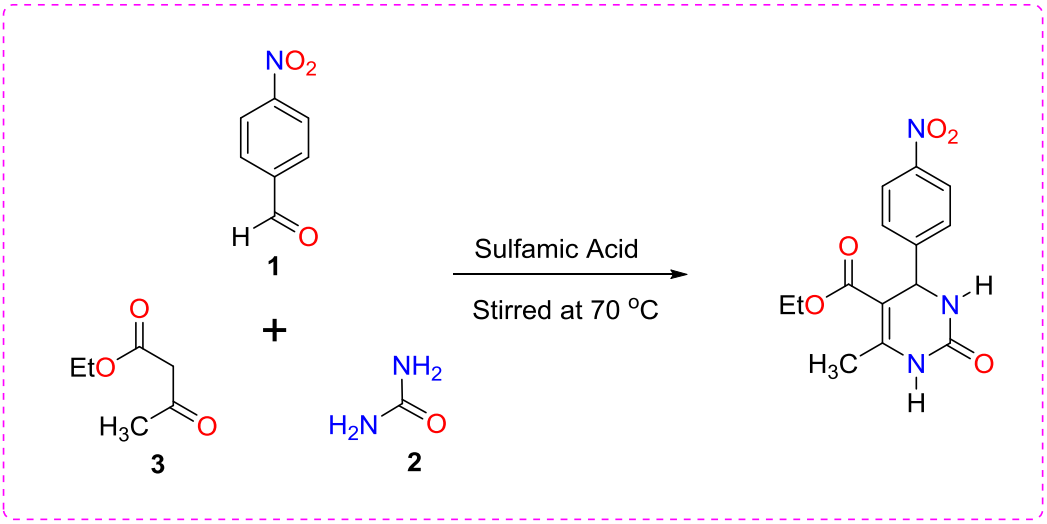

Scheme 1: Synthesis of titled compound.

2.3 Physical and spectral data for synthesized compound

Ethyl 6-methyl-4-(4-nitrophenyl)-2-oxo-1, 2, 3, 4-tetrahydropyrimidine-5-carboxylate (EMNTPC)

White colour; Yield 90%;FT-IR (KBr, cm^{-1}):3487.78, 3400.37, 3227.67, 3114.99, 2984.44, 2650.78, 2438.05, 1927.82, 1724.92, 1699.23, 1639.51, 1516.94, 1461.14, 1425.55, 1347.18, 1295.49, 1211.76, 1086.94, 1014.53, 956.80, 858.33, 777.63, 695.34, 653.24, 599.64

524.28.;^{1}H NMR (500 MHz, DMSO-d_6) δ 9.36 (s, 1H), 8.24 – 8.21 (m, 2H), 7.89 (d, J = 3.4 Hz, 1H), 7.54 – 7.50 (m, 2H), 5.29 (d, J = 3.4 Hz, 1H), 4.00 (q, J = 7.1 Hz, 2H), 2.28 (s, 3H), 1.10 (t, J = 7.0 Hz, 3H).; ^{13}C NMR (126 MHz, DMSO) δ 165.53, 152.47, 152.23, 149.86, 147.19, 128.13, 124.30, 98.65, 59.86, 54.16, 18.34, 14.51.

2.4 Computational details

Density Functional Theory (DFT) computations were performed using the Gaussian 09 suite on an Intel® Core™ i5 system, with no restrictions applied to the molecular geometry.[27] The hybrid functional B3LYP in combination with the 6-311++G(d,p) basis set was utilized to examine optimized molecular geometries, bond lengths, bond angles, atomic charges, and vibrational frequencies. Molecular structures obtained after optimization were visualized with the aid of GaussView 4.1 software. All calculations were carried out in the gas phase employing the 6-311++G(d,p) basis set to achieve detailed structural insights. From these studies, several physicochemical and electronic descriptors were derived, including total energy, electron distribution, chemical potential (μ), HOMO–LUMO energy levels and electron density, global hardness (η), softness (σ), electronegativity (χ), electrophilicity index (ω), and maximum charge transfer capability (ΔNmax).

2.4 ADME Study

The pharmacokinetic profile of possible drug candidates is assessed during the drug development process in large part by the ADME (Absorption, Distribution, Metabolism, and Excretion) analysis. The Molecular Modeling Group at the Swiss Institute of Bioinformatics (SIB) created the free web-based platform SwissADME, which offers a wide range of tools and predictive models for evaluating medicinal chemistry appropriateness, pharmacokinetics, and drug-likeness.[28] SwissADME enables early screening of compounds in the drug development pipeline by precisely predicting ADME features by utilizing molecular structures. The most promising candidates are selected for additional testing using this in silico method, which expedites the procedure and raises the possibility of clinical success. SwissADME calculates important metrics including hydrogen bond donors (HBDs) and acceptors (HBAs), rotatable bonds, solubility, and topological polar surface area (TPSA). Multiple logP calculations, such as iLOGP, XLOGP3, WLOGP, MLOGP, and SILICOS-IT, are incorporated into its lipophilicity estimates. These calculations are crucial for comprehending a molecule's capacity to pass through cell membranes. Another important factor influencing oral bioavailability is water solubility, which is also estimated by the tool.

In order to assess metabolism and possible drug-drug interactions, further anticipated ADME characteristics include gastrointestinal absorption, blood-brain barrier penetration, P-glycoprotein substrate status, and interactions with cytochrome P450 enzymes. The structural analysis also complies with Lipinski's "rule of five," which states that compound should have ten hydrogen bond acceptors and no more than five hydrogen bond donors. Furthermore, the TPSAwhich measures how much a molecule's surface is made up of polar fragmentsshould not be greater than 140 Å². Going above this limit could decrease membrane permeability and prevent the blood-brain barrier from penetrating.[29]

2.5 Molecular docking studies

Molecular docking is a pivotal technique in modern drug discovery, providing detailed insights into the interactions between small molecules (ligands) and their biological targets. In the present study, docking simulations were carried out using AutoDockTools 1.5.6,[30] which included steps such as protein and ligand preparation, grid box generation, and docking execution. Ligand geometries were stabilized via energy minimization at the MM2 level using Chem3D Pro.[31] The three-dimensional crystal structures of proteins were sourced from the Protein Data Bank (https://www.rcsb.org/). To further explore binding dynamics, 2D and 3D ligand-receptor interactions were visualized and analyzed with Discovery Studio Visualizer (DSV).[32]

3. RESULTS AND DISCUSSION

3.1 Chemistry

The NMR data of **EMNTPC** are consistent with its proposed structure.The FT-IR spectrum shows characteristic absorption bands confirming the functional groups: a broad band at 3487–3227 cm^{-1} corresponds to the NH stretching of the pyrimidine ring, while bands at 1724.92 and 1699.23 cm^{-1} indicate the ester and ketone carbonyl groups, respectively. The aromatic C=C stretching vibrations appear at 1639.51 and 1516.94 cm^{-1}, and the nitro group is confirmed by strong absorptions at 1347.18 and 1295.49 cm^{-1}. Additional bands at 1211.76 and 1086.94 cm^{-1} correspond to C–O stretching of the ester, and bands in the range 956.80–599.64 cm^{-1} indicate aromatic and skeletal C–H bending. The ^{1}H NMR spectrum shows a singlet at δ 9.36 ppm corresponding to the pyrimidine NH proton, while the pyrimidine ring protons at C5 and C6 appear as doublets at δ 7.89 and 5.29 ppm (J = 3.4 Hz), indicating vicinal coupling. The aromatic protons of the para-substituted 4-nitrophenyl group resonate as multiplets at δ 8.24–8.21 and 7.54–7.50 ppm. The ethyl ester group is evidenced by a

quartet at δ 4.00 ppm (CH_2) and a triplet at δ 1.10 ppm (CH_3), and the methyl group at C6 of the tetrahydropyrimidine ring appears as a singlet at δ 2.28 ppm. The ^{13}C NMR spectrum shows characteristic signals at δ 165.53 ppm for the ester carbonyl, δ 152–149 ppm for pyrimidine carbons, δ 128–124 ppm for aromatic carbons, δ 98.65 ppm for C5 of the ring, δ 59.86 and 14.51 ppm for the ethyl CH_2 and CH_3, δ 54.16 ppm for C6, and δ 18.34 ppm for the methyl group. Collectively, these spectral features confirm the presence of the tetrahydropyrimidine core, the 4-nitrophenyl substituent, and the ethyl ester moiety, in agreement with the assigned structure.

3.2 Computational study

3.2.1 Molecular structures

The synthesized compound **EMNTPC** was theoretically analyzed to evaluate various structural and chemical properties using DFT approach with the B3LYP functional and the 6-311++G(d,p) basis set.

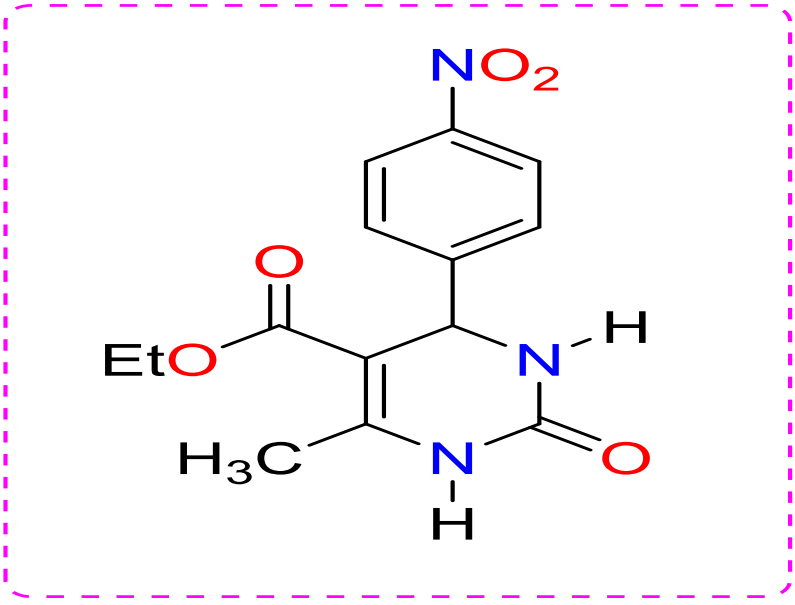

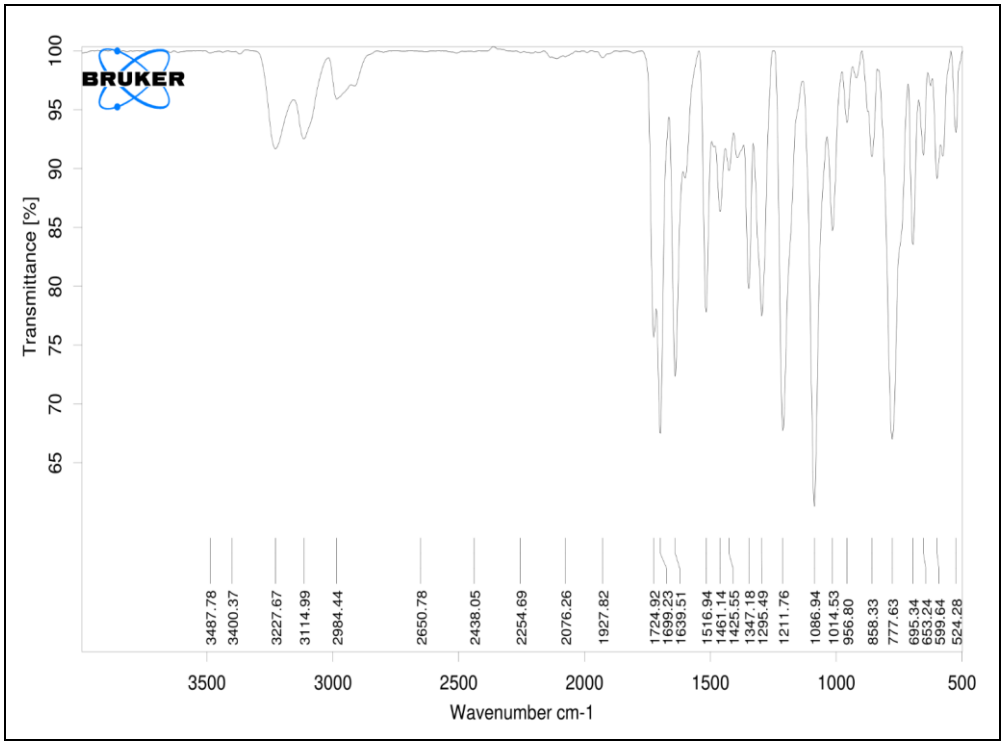

Fig. 1: FT-IR spectrum of EMNTPC.

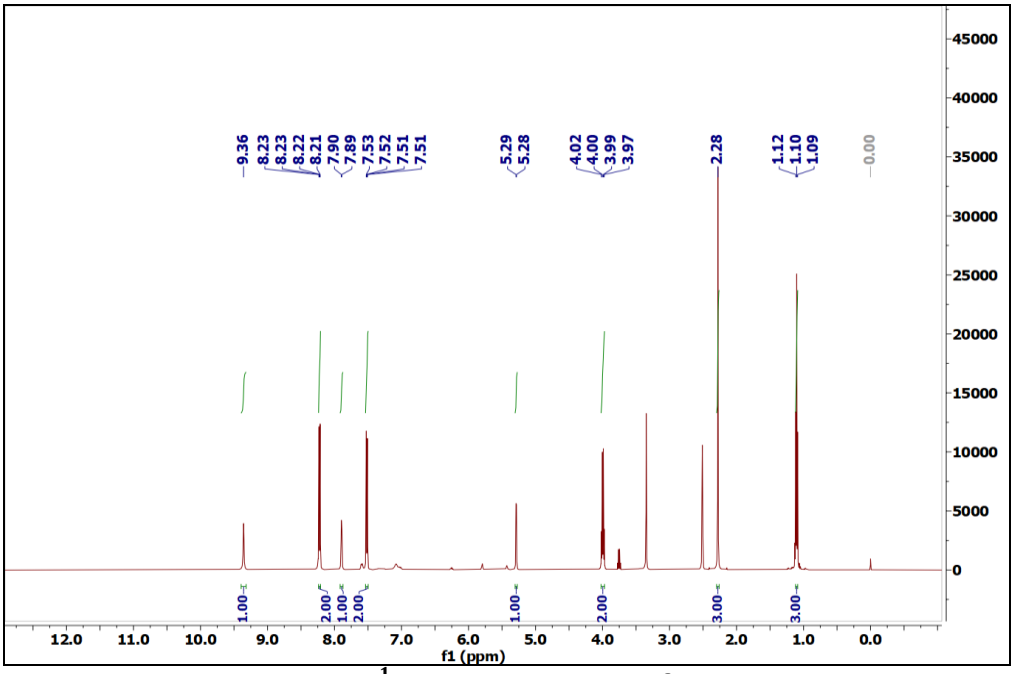

Fig. 1: ^{1}H NMR spectrum of EMNTPC.

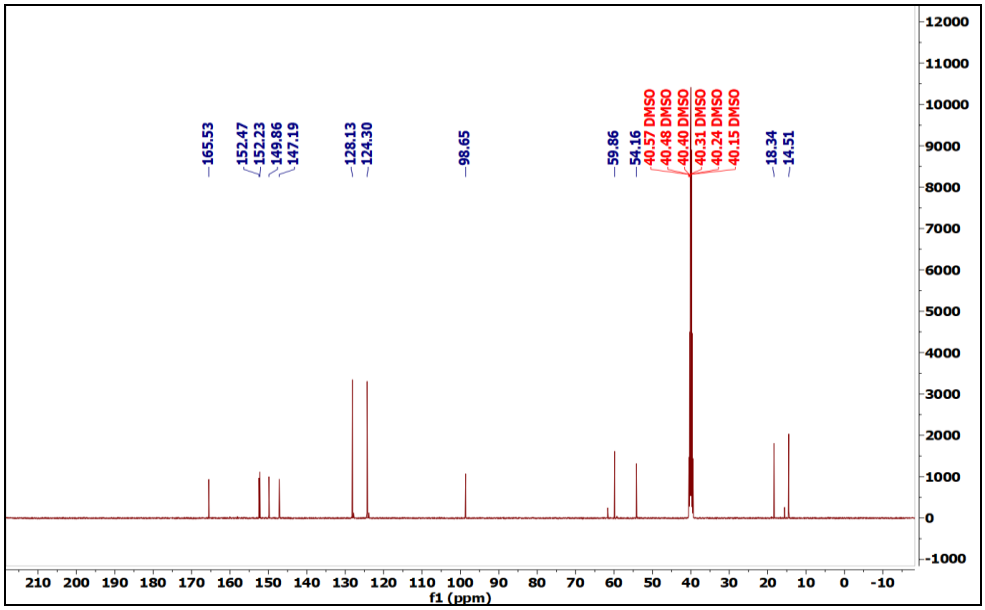

Fig. 2: ^{13}C NMR spectrum of EMNTPC.

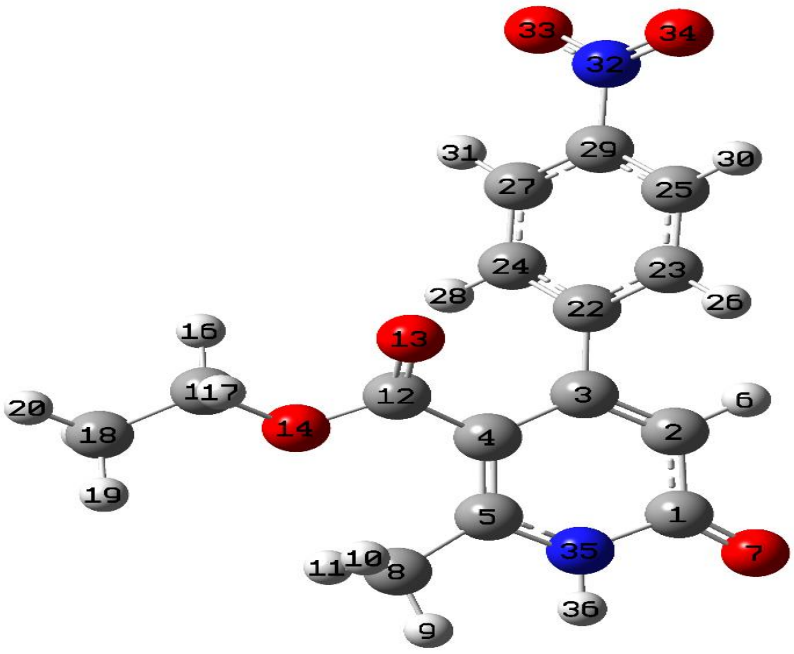

Fig. 1: Optimized structure of EMNTPC.

The structural parameters, including bond lengths (Å) and bond angles (°), of the optimized structure were computed using the DFT method for the **EMNTPC**. Although the molecular structures exhibit an overall asymmetrical nature, the computationally optimized geometries, as depicted in **Fig. 1**, reveal that the compound conforms to the C1 point group symmetry. Detailed information on the bond lengths and bond angles for the titled compound is provided in **Table 1** and **2**.

Table 1: Optimized geometrical parameter bond Length (Å) of compound EMNTPCby DFT/ B3LYP with 6-311++G(d,p) basis set.

Bond	Length (Å)	Bond	Length (Å)
C1−C2	1.4434	C15−C18	1.5147
C1−O7	1.2183	C18−H19	1.0923
C1−N35	1.414	C18−H20	1.093
C2−C3	1.3655	C18−H21	1.0922
C2−H6	1.0817	C22−C23	1.3989
C3−C4	1.4481	C22−C24	1.4008
C3−C22	1.4933	C23−C25	1.3892
C4−C5	1.3839	C23−H26	1.083
C4−C12	1.4877	C24−C27	1.3869
C5−C8	1.5064	C24−H28	1.0836
C5−N35	1.359	C25−C29	1.3892
C8−H9	1.0918	C25−H30	1.0809
C8−H10	1.0885	C27−C29	1.3909
C8−H11	1.0913	C27−H31	1.0809
C12−O13	1.2079	C29−N32	1.4778
C12−O14	1.3542	N32−O33	1.2242
O14−C15	1.452	N32−O34	1.2238
C15−H16	1.0918	N35−H36	1.0125
C15−H17	1.0924		

The bond length analysis reveals that the pyrimidine core exhibits C–C and C–N distances in the range of 1.36–1.44 Å, which lie between typical single and double bonds, reflecting strong π-electron delocalization and resonance stabilization. The C1–O7 bond (1.218 Å) is characteristic of a carbonyl double bond, whereas the C1–N35 bond (1.414 Å) indicates partial double-bond character due to conjugation. In the ester group, the C12–O13 bond (1.208 Å) is short, corresponding to the carbonyl oxygen, while the longer C12–O14 (1.354 Å) and O14–C15 (1.452 Å) distances represent C–O single bonds shortened by conjugation with the adjacent carbonyl. The nitro group shows nearly identical N–O bond lengths (1.224 Å each), confirming resonance delocalization, and the C29–N32 bond (1.478 Å) is slightly elongated due to the electron-withdrawing nature of the nitro substituent. The phenyl ring maintains uniform C–C bond lengths (~1.39 Å), consistent with aromatic stabilization, while aliphatic substituents such as C5–C8 (1.506 Å) and C15–C18 (1.515 Å) exhibit normal sp^3 C–C single bond distances, and all C–H bonds fall within the expected ~1.09 Å range.The bond angle data further complement these findings. Around the carbonyl carbon (C1), the angles C2–C1–O7 (127.7°), C2–C1–N35 (112.6°), and O7–C1–N35 (119.7°) confirm sp^2 hybridization with delocalization across the C=O and C–N bonds. The pyrimidine ring shows

internal angles close to 120° (e.g., C1–C2–C3, 122.4°; C2–C3–C4, 120.8°; C3–C4–C5, 118.2°), confirming its nearly planar conjugated geometry. In the ester group, bond angles such as C4–C12–O13 (124.1°), C4–C12–O14 (113.2°), and O13–C12–O14 (122.7°) align with a resonance-stabilized carboxylate system. The nitro substituent exhibits symmetric geometry with angles C29–N32–O33 (117.6°), C29–N32–O34 (117.6°), and O33–N32–O34 (124.8°), further supporting resonance delocalization. The phenyl ring maintains aromatic character with nearly uniform angles (~120°), while the aliphatic regions (C15, C18, C8) display tetrahedral angles between 107° and 112°, typical of sp^3 centers.Together, the bond length and bond angle results establish that **EMNTPC** possesses a partially planar, highly conjugated framework spanning the pyrimidine, ester, and nitrophenyl moieties, complemented by localized tetrahedral geometries in the aliphatic segments. This structural arrangement enhances resonance stabilization, modulates electronic distribution, and may play a key role in governing the compound's reactivity and biological interactions.

Table 2: Optimized geometrical parameter bond angle (°) of compound EMNTPC by DFT/ B3LYP with 6-311++G(d,p) basis set.

Angle	Value (°)	Angle	Value (°)
C2−C1−O7	127.6976	C4−C12−O14	113.1919
C2−C1−N35	112.5547	C13−C12−O14	122.7195
O7−C1−N35	119.7445	C12−C14−C15	115.7383
C1−C2−C3	122.4269	C14−C15−H16	108.4904
C1−C2−H6	116.2737	C14−C15−H17	108.7217
C3−C2−H6	121.2625	C14−C15−C18	107.6271
C2−C3−C4	120.8135	H16−C15−H17	107.5648
C2−C3−C22	117.2987	H16−C15−C18	112.0822
C4−C3−C22	121.7889	H17−C15−C18	112.2548
C3−C4−C5	118.2104	C15−C18−H19	111.2763
C3−C4−C12	118.9961	C15−C18−H20	109.6511
C5−C4−C12	122.4813	C15−C18−H21	110.9326
C4−C5−C8	126.5547	H19−C18−H20	108.1422
C4−C5−N35	118.697	H19−C18−H21	108.5052
C8−C5−N35	114.7389	H20−C18−H21	108.2387
C5−C8−H9	110.3272	C3−C22−C23	120.2911
C5−C8−H10	111.4586	C3−C22−C24	120.4115
C5−C8−H11	110.5375	C23−C22−C24	119.1814
H9−C8−H10	108.5866	C22−C23−C25	120.7148
H9−C8−H11	108.8275	C22−C23−H26	119.5614
H10−C8−H11	106.9996	C25−C23−H26	119.7143
C4−C12−O13	124.0874	C22−C24−C27	120.7414
C1−N35−C5	127.2742	C22−C24−H28	119.7599
C1−N35−H36	113.5272	C27−C24−H28	119.4951
C5−N35−H36	119.1793	C23−C25−C29	118.7419

C23−C25−H30	121.7595	C29−C25−H30	119.4986
C24−C27−C29	118.7392	C24−C27−H31	121.7998
C29−C27−H31	119.4609	C25−C29−C27	121.8774
C25−C29−N32	119.1	C27−C29−N32	119.0224
C29−N32−O33	117.5909	C29−N32−O34	117.631
O33−N32−O34	124.7781	-	-

3.2.2 Frontier molecular orbitals' and global descriptors' study

Frontier molecular orbitals provide valuable insight into the electronic structure and reactivity of molecules.[33] The HOMO represents the highest occupied orbital and indicates the electron-donating capacity, while the LUMO corresponds to the lowest unoccupied orbital and reflects the electron-accepting tendency. The relative energies of these orbitals determine how the molecule interacts with electrophiles and nucleophiles. The HOMO–LUMO energy gap (E_g) is a key descriptor of chemical behaviour, where a larger E_g indicates higher stability and lower reactivity, while a smaller E_g favours electron transfer, enhanced reactivity, and stronger biological interactions. Thus, E_{HOMO}, E_{LUMO}, and E_g collectively reflect the balance between stability and reactivity, offering theoretical support for understanding the molecule's potential chemical and biological activities. The frontier molecular orbitals namely HOMO and LUMO with energy gap (E_g) are depicted in **Fig. 2**.

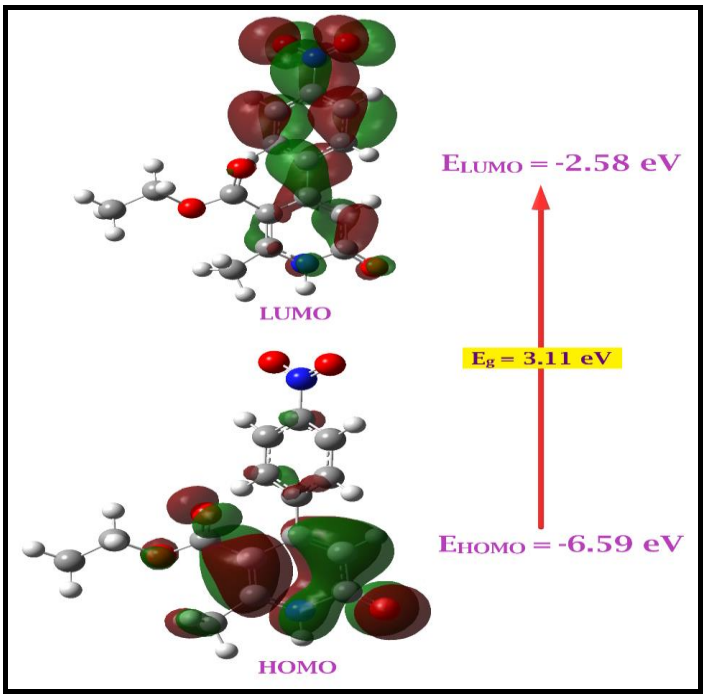

Fig. 2: The FMO's of compound EMNTPC with energy gap (E_g).

The electronic parameters of the compounds offer valuable information about their electronic structures and potential reactivity. The electronic parameters for compound **EMNTPC** are presented in **Table 3**.

Table 3: Electronic parameters of the EMNTPC.

E (a.u.)	-1065.86
E_{HOMO} (eV)	-6.59
E_{LUMO} (eV)	-2.58
I (eV)	6.59
A (eV)	2.58
E_g(eV)	4.09
Dipole moment (Debye)	8.2026

Using Koopmans' theorem, the global reactivity descriptors of the synthesized compound were computed[34] and are given in **Table 4**.

Table 4: Global reactivity parameters of EMNTPC.

Chemical Hardness η (eV)	2.00 eV
Chemical Softness σ (eV^{-1})	0.49eV^{-1}
Electronegativity χ (eV)	4.85 eV
Chemical Potential μ (eV)	-4.85 eV
Global Electrophilicity ω (eV)	5.25 eV
Maximum Electronic ChargeΔNmax	2.29

η=chemical hardness; σ, chemical softness; ω, global electrophilicity; χ, electronegativity; μ, chemical potential; ΔNmax=maximum electronic charge.

The electronic properties of Ethyl 6-methyl-4-(4-nitrophenyl)-2-oxo-1,2,3,4-tetrahydropyrimidine-5-carboxylate (**EMNTPC**) were analyzed using density functional theory (DFT) calculations. The total electronic energy of the molecule was found to be -1065.86 a.u., indicating a stable ground-state structure. The HOMO (Highest Occupied Molecular Orbital) energy of -6.59 eV and the LUMO (Lowest Unoccupied Molecular Orbital) energy of -2.58 eV correspond to an energy gap (Eg) of 4.09 eV, suggesting moderate chemical stability and reactivity. A large energy gap generally correlates with lower chemical reactivity, while a smaller gap indicates higher polarizability and reactivity. The ionization potential (I = 6.59 eV) and electron affinity (A = 2.58 eV) were derived from the HOMO and LUMO energies, reflecting the molecule's ability to donate or accept electrons. The computed dipole moment of 8.2026 D indicates significant molecular polarity, which may enhance interactions with polar solvents or biological targets.

Using Koopmans' theorem, global reactivity descriptors were calculated to assess the chemical behavior of **EMNTPC**. The chemical hardness (η = 2.00 eV) and softness (σ = 0.49 eV^{-1}) suggest a moderate resistance to electron cloud deformation, with reasonable reactivity toward electrophilic and nucleophilic species. The electronegativity (χ = 4.85 eV) and chemical potential (μ = -4.85 eV) indicate a tendency to attract electrons and stabilize electronic distribution. The global electrophilicity index (ω = 5.25 eV) highlights the molecule's ability to accept electrons, suggesting potential interactions with nucleophilic sites in biological targets. Finally, the maximum electronic charge transfer (ΔNmax = 2.29) reflects the compound's capacity to exchange electrons during chemical interactions. Collectively, these electronic and reactivity parameters reveal that **EMNTPC** possesses a balanced profile of stability and moderate chemical reactivity, which could be favorable for its interactions in biological systems and potential pharmacological activity.

3.2.3 Mulliken atomic charges

Mulliken atomic charge analysis is a widely used method to evaluate the electronic distribution within a molecule. By partitioning the electron density among constituent atoms, it provides insights into charge polarization, electron-rich and electron-deficient sites, and the overall electronic environment. Such information is crucial for understanding molecular stability, predicting reactive centers, and rationalizing non-covalent interactions, including hydrogen bonding and electrostatic forces. Derived from Mulliken population analysis, these charges are calculated from the electron density obtained in computational simulations, allowing precise identification of electron-rich and electron-deficient regions within the molecule.

Table 5: Mulliken atomic charges of EMNTPC.

Atom	Charge	Atom	Charge
C1	0.413789	H19	0.113246
C2	-0.22925	C20	0.116677
C3	0.151986	H21	0.117816
C4	-0.25963	C22	-0.0752
C5	0.292125	C23	-0.04861
H6	0.119305	C24	-0.02942
O7	-0.35652	C25	-0.0433
C8	-0.21415	H26	0.105807
H9	0.105453	C27	-0.04428
H10	0.142188	H28	0.1017
H11	0.15392	C29	0.120275
C12	0.323387	H30	0.13634

O13	-0.34148	H31	0.134417
O14	-0.35311	N32	0.17139
C15	-0.02163	O33	-0.27086
H16	0.126986	O34	-0.26898
H17	0.124651	N35	-0.44543
C18	-0.30417	H36	0.234544

Table 5 summarizes the Mulliken atomic charge distribution of the studied compound, highlighting the electronic environment around different atoms. As expected, electronegative atoms such as oxygen (O7, O13, O14, O33, and O34) and nitrogen (N35) carry significant negative charges, with N35 being the most negative (–0.445 e), indicating its strong electron-withdrawing nature and potential role as a reactive site for electrophilic attack. In contrast, most hydrogen atoms exhibit positive charges (0.10–0.23 e), reflecting their electron-deficient character and propensity for hydrogen bonding. Among the carbon atoms, variable charge distribution is observed: C1 (0.414 e), C5 (0.292 e), and C12 (0.323 e) possess notable positive charges, whereas C2 (–0.229 e), C4 (–0.260 e), and C18 (–0.304 e) carry negative charges, suggesting charge polarization within the ring and substituent framework. This uneven distribution of electron density provides valuable insights into intramolecular interactions, stability, and possible reactive centers of the molecule.

3.3 Molecular electrostatic potential surface analysis

Molecular electrostatic potential (MEP) mapping offers a detailed visualization of the electron density distribution across a molecule, allowing the identification of regions that are likely to participate in chemical interactions. Red-colored zones, indicating areas of high electron density, are typically located near electronegative atoms like oxygen and are prone to attack by electrophiles. In contrast, blue regions represent electron-deficient areas, which can readily interact with nucleophiles. Areas shown in green correspond to regions of relatively balanced electron density, suggesting minimal polarity. MEP analysis is instrumental in predicting sites for hydrogen bonding, reactive centers, and potential molecular interactions with enzymes or receptors. When integrated with frontier molecular orbital (FMO) data, it provides a spatial perspective of molecular reactivity, complementing energy-based electronic insights. This combined approach enhances the understanding of structure-activity relationships and supports rational drug design by correlating electron distribution with potential pharmacological behaviour. The MEP surface of **EMNTPC** is depicted in **Fig. 3**.

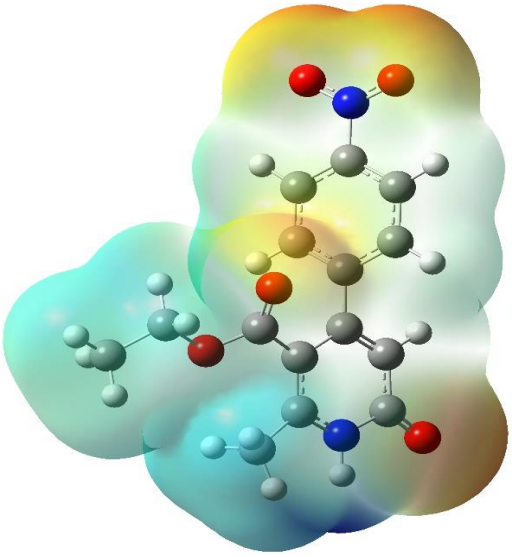

Fig. 3: Molecular electrostatic potential (EMNTPC).

The molecular electrostatic potential (MEP) surface highlights the distribution of electron density and reactive sites in the molecule. Red regions, located mainly on the nitro and carbonyl groups, indicate electron-rich areas susceptible to electrophilic attack and potential hydrogen-bonding interactions. Blue regions, particularly around hydrogen atoms bonded to nitrogen in the pyrimidine ring, denote electron-deficient sites favorable for nucleophilic interactions. Green and yellow areas over the tetrahydropyrimidine ring and ethyl ester moiety suggest moderate polarity and relative chemical stability. Overall, the MEP map provides a clear visualization of reactive regions, complementing frontier molecular orbital analysis to predict chemical reactivity, ligand binding, and potential biological interactions.

3.4 ADME study

Some ADME (Absorption, Distribution, Metabolism, and Excretion) parameters of the compound **EMNTPC** were studied and in **Table 6**, which were calculated by SwissADME. The ADME parameters of the synthesized compounds, exhibit a range of physicochemical properties that influence their pharmacokinetics. The bioavailability radar plots and BOILED-Egg plots of **EMNTPC**is depicted in Fig. 4.

Table 6: The ADME Parameters of compoundEMNTPC.

Parameters	Values
Number of Hydrogen bond donors (nHD)	2
Number of Hydrogen bond acceptors (nHA)	5
Molecular Polar surface area (TPSA), Å2	113.25

Consensus Log Po/w	0.81
Log S (ESOL)	-2.37
Water Solubility	Soluble
Gastrointestinal absorption	High
BBB permeability	No
P-gp substrate	No
Metabolic enzymes inhibition	No
Drug likeness matching	Lipinski, Ghose, Veber, Egan Muegge

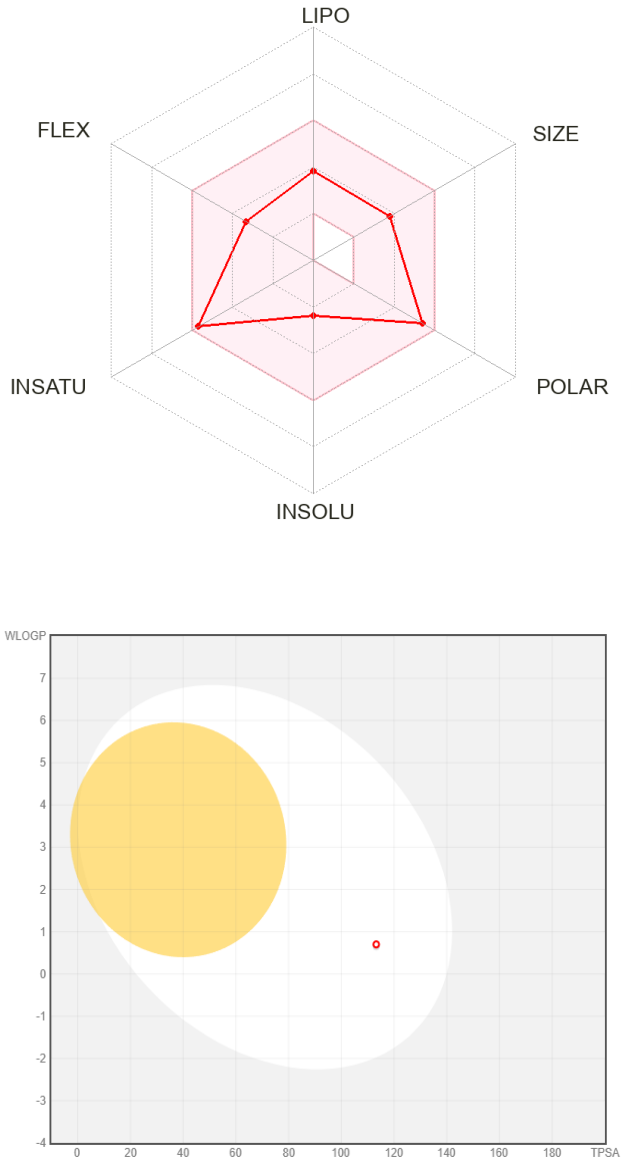

Fig. 4: Bioavailability radar plots and BOILED-Egg plots.

The ADME (Absorption, Distribution, Metabolism, and Excretion) profile of **EMNTPC** was evaluated to predict its pharmacokinetic properties. The compound possesses two hydrogen bond donors (nHD) and five hydrogen bond acceptors (nHA), which are within the favorable

range for oral bioavailability and indicate the potential for hydrogen bonding interactions with biological targets. The topological polar surface area (TPSA) of 113.25 Å² suggests adequate polarity, contributing to good solubility and absorption characteristics. The consensus Log P (Po/w) of 0.81 indicates moderate lipophilicity, favoring both solubility and membrane permeability, while the predicted aqueous solubility (Log S ESOL = -2.37; classified as soluble) supports satisfactory dissolution in biological fluids. The compound is predicted to have high gastrointestinal (GI) absorption, suggesting efficient oral uptake, but it is not permeable across the blood-brain barrier (BBB), indicating minimal central nervous system exposure. Importantly, **EMNTPC** is not a substrate of P-glycoprotein (P-gp) and does not inhibit major metabolic enzymes, reducing the likelihood of efflux-related resistance and drug-drug interactions. Furthermore, the compound complies with multiple drug-likeness rules, including Lipinski, Ghose, Veber, Egan, and Muegge filters, indicating favorable pharmacokinetic and drug-like properties. Collectively, these ADME predictions suggest that **EMNTPC** has promising oral bioavailability, suitable solubility, and a favorable pharmacokinetic profile, making it a viable candidate for further preclinical development.

3.5 Molecular docking study

To investigate the plausible interactions of the synthesized scaffold and theoretically assess its antimicrobial potential, a molecular docking study was performed against two distinct protein targets: sterol 14-α demethylase (CYP51) from *Candida albicans* (PDB ID: 5TZ1) and the DNA GyrB subunit of *Escherichia coli* (PDB ID: 6YD9). These targets were selected based on their clinical relevance and established roles as antimicrobial drug targets. CYP51 is a crucial enzyme in fungal ergosterol biosynthesis and a well-known target of azole antifungals, while DNA gyrase is essential for bacterial DNA replication, with GyrB serving as a validated antibacterial target exploited by fluoroquinolone antibiotics. Both proteins have available high-resolution crystal structures in the Protein Data Bank, ensuring suitability for reliable docking simulations. Molecular docking of **EMNTPC** into the active site of CYP51 revealed a binding affinity of –8.2 kcal/mol, while docking into the *E. coli* GyrB24 domain yielded a binding affinity of –6.7 kcal/mol, both indicating stable and energetically favorable interactions.The detailed binding interactions, including the involved residues and types of interactions, are summarized in **Table 7**.

Table 7: Molecular docking scores and key binding interactions of EMNTPC with selected protein targets.

PDB ID	Docking Score (kcal/mol)	Key Interactions
5TZ1	–8.2	Conventional hydrogen bond with TYR132; Carbon–hydrogen bond with ILE304; π–Donor hydrogen bond with TYR118; Hydrophobic and π–alkyl interactions with PHE228 and HIS310; π–Alkyl interaction with HEM601 (heme group).
6YD9	–6.7	π–Cation interaction with ARG76; π–Anion interaction with GLU50; Alkyl interaction with ILE94; π–Alkyl interaction with ILE78.

The docking analysis of Ethyl 6-methyl-4-(4-nitrophenyl)-2-oxo-1,2,3,4-tetrahydropyrimidine-5-carboxylate with CYP51 demonstrated a network of stabilizing interactions within the active site. A strong conventional hydrogen bond was formed between TYR132 and the ligand oxygen atom, serving as a key anchoring interaction, while additional hydrogen bonding was established with ILE304 through a carbon–hydrogen bond and with TYR118 via a π-donor hydrogen bond. These interactions collectively enhanced the stability of the ligand within the binding pocket. Hydrophobic stabilization was also observed, with PHE228 and HIS310 engaging in π–alkyl contacts. Importantly, the ligand displayed a π–alkyl interaction with the heme group (HEM601), a feature crucial for inhibitory activity since CYP51 inhibitors typically disrupt enzyme function by directly engaging the heme pocket. These findings suggest that the compound is well accommodated within the CYP51 active site and holds potential to act as an antifungal agent by interfering with ergosterol biosynthesis.Similarly, docking with the DNA gyrase B subunit of *E. coli* revealed that the compound engages in both electrostatic and hydrophobic interactions. Electrostatic stabilization was evident through a π–cation interaction with ARG76 and a π–anion interaction with GLU50, reflecting the compound's ability to interact with charged residues in the binding pocket. Additional hydrophobic contacts, including an alkyl interaction with ILE94 and a π–alkyl interaction with ILE78, further reinforced ligand stability within the active site. Together, these interactions suggest that the compound binds favorably to DNA gyrase B, potentially interfering with its enzymatic function and contributing to antibacterial activity.The binding interactions of **EMNTPC** with *E. coli* DNA GyrB (PDB ID: 6YD9) and sterol 14-α demethylase from *C. albicans* (PDB ID: 5TZ1) are illustrated in **Fig. 5** and **6**, respectively.

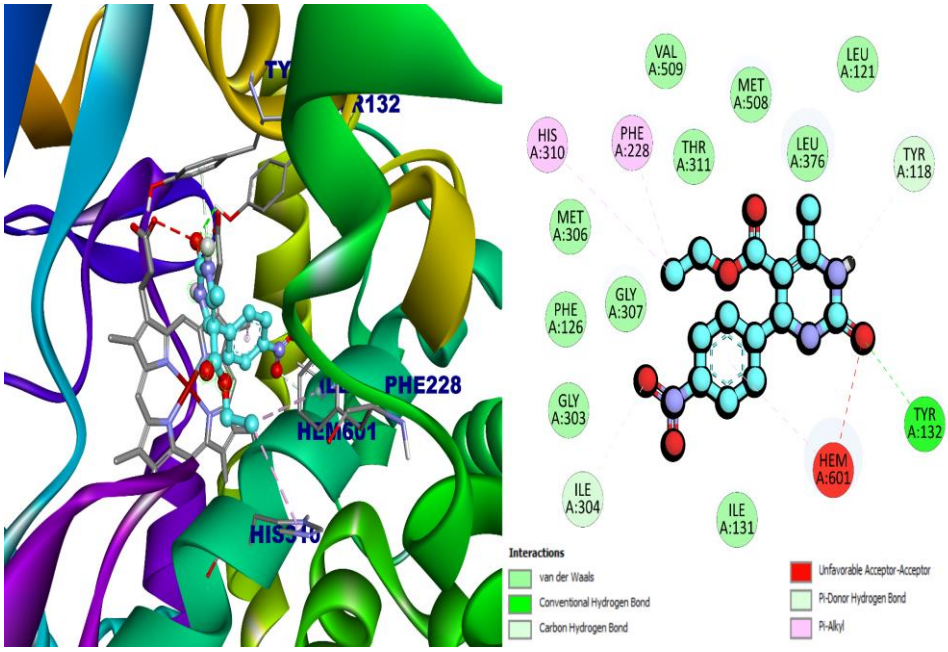

Fig. 5: Binding interactions of EMNTPC with sterol 14-α demethylase (CYP51) from *C. albicans* (PDB ID: 5TZ1).

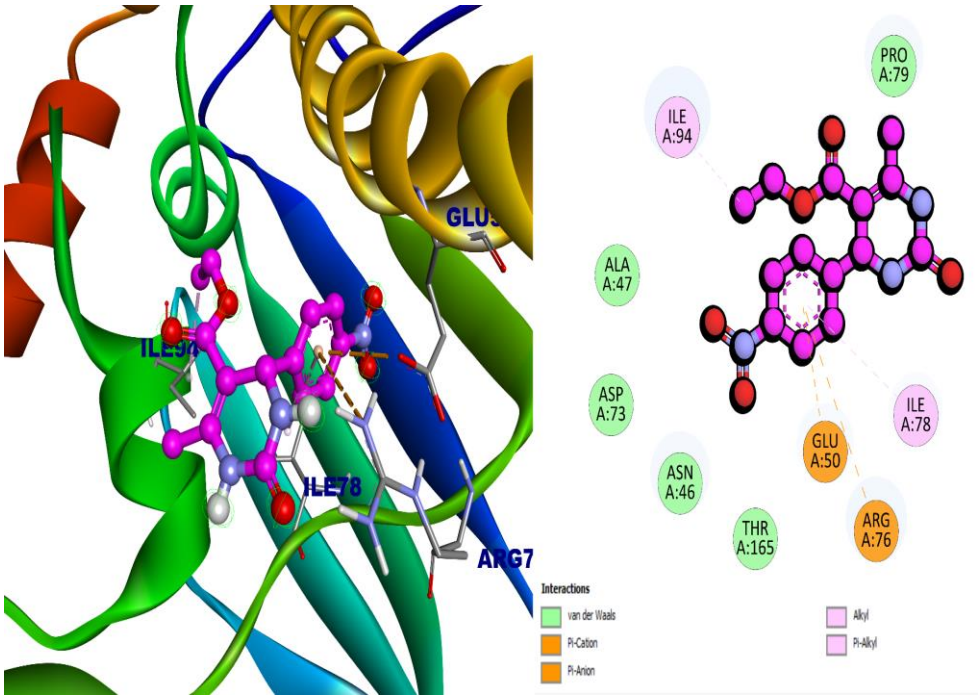

Fig. 6: Bindinginteraction of EMNTPC with *E. coli* DNA GyrB(PDB ID: 6YD9).

4. CONCLUSION

In this study, a 3,4-dihydropyrimidine-2(1*H*)-one derivative was successfully synthesized via a one-pot condensation strategy using sulfamic acid as a green and efficient catalyst. Structural characterization through FT-IR, ^{1}H and ^{13}C NMR confirmed the formation of the

target compound. Density Functional Theory (DFT) studies provided detailed insights into the optimized molecular geometry, bond parameters, revealing a partially planar, conjugated framework with resonance stabilization across the pyrimidine, ester, and nitrophenyl units. Frontier molecular orbital analysis indicated a HOMO–LUMO energy gap of 4.09 eV, reflecting moderate chemical reactivity, while molecular electrostatic potential mapping highlighted reactive electron-rich and electron-deficient sites. In silico ADME evaluation predicted favorable pharmacokinetic properties, including good solubility, high gastrointestinal absorption, and compliance with Lipinski's rule of five. Molecular docking studies demonstrated strong and stable interactions with sterol 14-α demethylase (CYP51) and *E. coli* DNA gyrase B, including key hydrogen bonding, π–donor hydrogen bonding, π–cation, π–anion, and hydrophobic contacts, suggesting potential antifungal and antibacterial activity. Collectively, these findings indicate that the synthesized compound possesses a balanced combination of structural stability, moderate reactivity, favorable pharmacokinetics, and promising biological activity, making it a valuable scaffold for further medicinal chemistry and drug development studies.

ACKNOWLEDGEMENTS

The author acknowledge central instrumentation facility (CIF), Savitribai Phule Pune University, Pune for NMR analysis and CIC, KTHM College for FT-IR analysis. Authors also would like to acknowledge MGV's Maharaja SayajiraoGaikwad Arts, Science & Commerce College, Malegaon Camp Nashik (India) for providing necessary research facilities.

Data availability: No datasets were generated or analyzed during the current study.

DECLARATIONS

Funding Declaration

The authors did not receive support from any organization for the submitted work.

Ethics approval and consent to participate

All the authors have read and agreed to the ethics for publishing the manuscript.

Consent for publication

All authors have consented to publish this work.

Competing interests

The authors declare no competing interests.

REFERENCES

1. Gajic, I., Tomic, N., Lukovic, B., Jovicevic, M., Kekic, D., Petrovic, M., Jankovic, M., Trudic, A., MiticCulafic, D., Milenkovic, M. and Opavski, N., A comprehensive overview of antibacterial agents for combating Multidrug-Resistant bacteria: the current landscape, development, future opportunities, and challenges. *Antibiotics*, 2025; *14*(3): 221.
2. Terreni, M., Taccani, M. and Pregnolato, M., New antibiotics for multidrug-resistant bacterial strains: latest research developments and future perspectives. *Molecules*, 2021; *26*(9): 2671.
3. Almutairy, B., Extensively and multidrug-resistant bacterial strains: case studies of antibiotics resistance. *Frontiers in Microbiology*, 2024; *15*: 1381511.
4. Shinde, R.A., Adole, V.A., Jagdale, B.S. and Pawar, T.B., Superfast synthesis, antibacterial and antifungal studies of halo-aryl and heterocyclic tagged 2, 3-dihydro-1 H-inden-1-one candidates. *MonatsheftefürChemie-Chemical Monthly*, 2021; *152*(6): 649-658.
5. Ebenezer, O., Jordaan, M.A., Carena, G., Bono, T., Shapi, M. and Tuszynski, J.A., An overview of the biological evaluation of selected nitrogen-containing heterocycle medicinal chemistry compounds. *International Journal of Molecular Sciences*, 2022; *23*(15): 8117.
6. Kerru, N., Gummidi, L., Maddila, S., Gangu, K.K. and Jonnalagadda, S.B., A review on recent advances in nitrogen-containing molecules and their biological applications. *Molecules*, 2020; *25*(8): 1909.
7. Frank, É. and Szőllősi, G., Nitrogen-containing heterocycles as significant molecular scaffolds for medicinal and other applications. *Molecules*, 2021; *26*(15): 4617.
8. Wan, J.P. and Pan, Y., Recent advance in the pharmacology of dihydropyrimidinone. *Mini Reviews in Medicinal Chemistry*, 2012; *12*(4): 337-349.

9. Khasimbi, S., Ali, F., Manda, K., Sharma, A., Chauhan, G. and Wakode, S., Dihydropyrimidinones scaffold as a promising nucleus for synthetic profile and various therapeutic targets: A Review. *Current Organic Synthesis*, 2021; *18*(3): 270-293.
10. Ramachandran, V., Arumugasamy, K., Singh, S.K., Edayadulla, N., Ramesh, P. and Kamaraj, S.K., Synthesis, antibacterial studies, and molecular modeling studies of 3, 4-dihydropyrimidinone compounds. *Journal of chemical biology*, 2016; *9*(1): 31-40.
11. deAzambuja, G.O., Svetaz, L., Gonçalves, I.L., Corbelini, P.F., von Poser, G.L., Kawano, D.F., Zacchino, S. and Eifler-Lima, V.L., In vitro antifungal activity of dihydropyrimidinones/thiones against *Candida albicans* and Cryptococcus neoformans. *Current Bioactive Compounds*, 2019; *15*(6): 648-655.
12. Prasad, T., Mahapatra, A., Sharma, T., Sahoo, C.R. and Padhy, R.N., Dihydropyrimidinones as potent anticancer agents: Insight into the structure–activity relationship. *Archiv der Pharmazie*, 2023; *356*(6): 2200664.
13. Nawal, N., Chawla, P.A., Virendra, S.A. and Chawla, V., 3, 4-Dihydropyrimidine-2 (1 H)-one/thione derivatives as anti-inflammatory and antioxidant agents: synthesis, biological activity, and docking studies. *Current Organic Chemistry*, 2025; *29*(10): 814-832.
14. Stefani, H.A., Oliveira, C.B., Almeida, R.B., Pereira, C.M., Braga, R.C., Cella, R., Borges, V.C., Savegnago, L. and Nogueira, C.W., Dihydropyrimidin-(2H)-ones obtained by ultrasound irradiation: a new class of potential antioxidant agents. *European journal of medicinal chemistry*, 2006; *41*(4): 513-518.
15. Fauzi, A., Saifudin, A. and Rullah, K., Synthesis of Dihydropyrimidinone (DHPM) derivatives through a multicomponent reaction (MCR) and their biological activity. *Journal of Medicinal and Chemical Sciences*, 2023; *6*(8): 1810-1817.
16. Gupta, P.K., Pal, Y., Kumar, P., Gupta, S., Singh, S.D. and Tiwari, S.B., A Critical Review on Computational Techniques through in silico Assisted Drug Design. *International Journal of Pharmaceutical Investigation*, 2024; *14*(4).
17. Ouma, R.B., Ngari, S.M. and Kibet, J.K., A review of the current trends in computational approaches in drug design and metabolism. *Discover Public Health*, 2024; *21*(1): 108.
18. Babu, V., Ahmed, S., Rahiman, A.K., Kawsar, S.M., Berredjem, M., Bhat, A.R. and Basha, K.A., Computational chemistry: prediction of compound accessibility of targeted synthesized compounds. *Medicinal Chemistry*, 2025; *21*(5): 334-344.

19. Shinde, R.A., Adole, V.A., Jagdale, B.S. and Desale, B.S., Synthesis, antibacterial and computational studies of Halo Chalcone hybrids from 1-(2, 3-Dihydrobenzo [b][1, 4] dioxin-6-yl) ethan-1-one. *Journal of the Indian Chemical Society*, 2021; *98*(4): 100051.
20. Adole, V.A., More, R.A., Jagdale, B.S., Pawar, T.B., Chobe, S.S., Shinde, R.A., Dhonnar, S.L., Koli, P.B., Patil, A.V., Bukane, A.R. and Gacche, R.N., Microwave prompted solvent-free synthesis of new series of heterocyclic tagged 7-arylidene indanone hybrids and their computational, antifungal, antioxidant, and cytotoxicity study. *Bioorganic Chemistry*, 2021; *115*: 105259.
21. Shinde, R.A., Adole, V.A., Shinde, R.S., Desale, B.S. and Jagdale, B.S., Synthesis, antibacterial, antifungal and computational study of (E)-4-(3-(2, 3-dihydrobenzo [b][1, 4] dioxin-6-yl)-3-oxoprop-1-en-1-yl) benzonitrile. *Results in Chemistry*, 2022; *4*: 100553.
22. Shinde, R.A., Adole, V.A. and Jagdale, B.S., Antimicrobial and computational investigation of two 2, 3-dihydro-1 H-inden-1-one derived fluorinated chalcone motifs. *Vietnam Journal of Chemistry*, 2021; *59*(6): 800-812.
23. Sable, Y.R., Shinde, R.A., Yasin, H.K.A., Ghanwate, N., Mali, S.N., Ghotekar, S.K., Gawari, D.P., Sasane, D.A. and Adole, V.A., Furan–thiazolehydrazone scaffolds as promising antitubercular and antibacterial agents: synthesis, characterization, bioevaluation and computational analysis. *RSC advances*, 2025; *15*(36): 30001.
24. Sable, Y.R., Adole, V.A., Shinde, R.A., Deshmukh, H.S., Rajesh, R., Almutairi, T.M., Alam, M. and Islam, M.S., Exploring Pyrazole Integrated Thiazole Molecular Hybrids for Antitubercular Activity: Synthesis, Spectral Characterization, DFT, ADME, and Docking Studies. *Journal of Molecular Structure*, 2025; 142891.
25. Shinde, R.A., Adole, V.A., Patil, R.H., Khairnar, B.B., Jagdale, B.S., Almutairi, T.M., Patel, H., Islam, M.S., Ahmad, I., Kumar, A.R. and Selvaraj, S., Harnessing thiazole chemistry for antifungal strategies through an experimental and computational chemistry approach: anti-biofilm, molecular docking, dynamics, and DFT analysis. *RSC advances*, 2025; *15*(27): 21838-21858.
26. Adole, V.A., Kumar, A., Misra, N., Shinde, R.A. and Jagdale, B.S., Synthesis, computational, antimicrobial, antioxidant, and ADME study of 2-(3, 4-dimethoxyphenyl)-4 H-chromen-4-one. *Polycyclic Aromatic Compounds*, 2024; *44*(8): 5397-5411.
27. Frisch MJ, T., Schlegelhb, S., Robbma, C.J., Montgomery Jr, J.A., Vreven, T., Kudin, K.N.., Burant, J.C., Millam, J.M., Iyengar, S.S., Tomasi, J. and Barone, V., Gaussian 03, Revision C. 2004; 02.

28. Daina, A., Michielin, O. and Zoete, V., SwissADME: a free web tool to evaluate pharmacokinetics, drug-likeness and medicinal chemistry friendliness of small molecules. *Scientific reports*, 2017; *7*(1): 42717.
29. da Silva, C.P., das Neves, G.M., Poser, G.L.V., Eifler-Lima, V.L. and Rates, S.M.K., In silico Prediction of ADMET/Drug-likeness Properties of Bioactive Phloroglucinols from Hypericum Genus. *Medicinal Chemistry*, 2023; *19*(10): 1002-1017.
30. Trott, O. and Olson, A.J., AutoDockVina: improving the speed and accuracy of docking with a new scoring function, efficient optimization, and multithreading. *Journal of computational chemistry*, 2010; *31*(2): 455-461.
31. Alhawarri, M.B., Exploring the Anticancer Potential of Furanpydone A: A Computational Study on its Inhibition of MTHFD2 Across Diverse Cancer Cell Lines. *Cell Biochemistry and Biophysics*, 2024; 1-18.
32. Pitaloka, D.A.E., Ramadhan, D.S.F., Arfan, Chaidir, L. and Fakih, T.M., Docking-based virtual screening and molecular dynamics simulations of quercetinanalogs as enoyl-acyl carrier protein reductase (InhA) inhibitors of Mycobacterium tuberculosis. *ScientiaPharmaceutica*, 2021; *89*(2): 20.
33. Venkatesh, G., Vennila, P., Govindasamy, C., El Newehy, A.S., Mammadova, K., Mishma, J.C., Manikandan, A. and Balasubramaniyan, S., Synthesis, characterization, antiproliferative, antibacterial activity, RDG, ELF, LOL Molecular docking and physico chemical properties of novel benzodiazepine derivatives. *Journal of Molecular Structure*, 2025; *1322*: 140519.
34. T. Koopmans, Über die Zuordnung von Wellenfunktionen und Eigenwertenzu den einzelnenElektroneneines atoms, Physical 1934; (1-6): 104–113.